ARTICLE

Effect of Potassium Addition on Coprecipitated Iron Catalysts for Fischer-Tropsch Synthesis Using Bio-oil-syngas

Zhao-xiang Wang, Ting Dong, Tao Kan, Quan-xin Li*

Department of Chemical Physics, Lab of Biomass Clean Energy, University of Science and Technology of China, Hefei 230026, China

(Dated: Received on April 4, 2007; Accepted on August 6, 2007)

The effects of potassium addition and the potassium content on the activity and selectivity of coprecipitated iron catalyst for Fischer-Tropsch synthesis (FTS) were studied in a fixed bed reactor at 1.5 MPa, 300 °C, and contact time (W/F) of 12.5 $g_{cat}h$/mol using the model bio-oil-syngas of $H_2/CO/CO_2/N_2$ (62/8/25/5, vol%). It was found that potassium addition increases the catalyst activity for FTS and the reverse water gas shift reaction. Moreover, potassium increases the average molecular weight (chain length) of the hydrocarbon products. With the increase of potassium content, it was found that CH_4 selectivity decreases and the selectivity of liquid phase products (C_{5+}) increases. The characteristics of FTS catalysts with different potassium content were also investigated by various characterization measurements including X-ray diffraction, X-ray photoelectron spectroscopy and Brunauer-Emmett-Teller surface area. Based on experimental results, 100Fe/6Cu/16Al/6K (weight ratio) was selected as the optimal catalyst for FTS from bio-oil-syngas. The results indicate that the 100Fe/6Cu/16Al/6K catalyst is one of the most promising candidates to directly synthesize liquid bio-fuel using bio-oil-syngas.

Key words: Bio-oil-syngas, Fischer-Tropsch synthesis, Potassium, Coprecipitated iron

I. INTRODUCTION

Concerns about the depletion of fossil fuel reserves and the pollution caused by continuously increasing energy demands make biomass an attractive alternative energy source. Biomass is derived from numerous sources, including the by-products from the timber industry, agricultural crops, raw material from the forest, major parts of household waste and wood. Biomass does not add carbon dioxide to the atmosphere as it absorbs the same amount of carbon in growing as it releases when consumed as a fuel. Moreover, biomass can be used to generate electricity with the same equipment or power plants that are now burning fossil fuels. Biomass is an important source of energy and the most important fuel worldwide after coal, oil and natural gas.

Up to now, various technologies, e.g. catalytic pyrolysis of biomass [1,2], biomass gasification [3,4], and biochemical methods [5], have been explored to utilize biomass energy. For over two decades there has been an active effort in North America and Europe by many researchers, in both academia and industry, to develop better methods for producing alternative fuels from biomass by the use of pyrolytic technologies. The conversion of lignocellulosic materials to liquids oil (bio-oil) has been the process of greatest interest in many works [6,7], because liquid fuels appear to have the most general applicability as an alternative energy source. Bio-oil generally contains numerous oxygenated organic compounds including acids, alcohols, aldehydes, ketones, substituted phenolics and other complex oxygenates derived from biomass carbohydrates and lignin [8]. For the viewpoint of real application, bio-oil has many advantages such as collection, transportation and storage. At the same time, it also has some disadvantages for utilizing bio-oil directly. Since most bio-oils are polar, viscous, and corrosive and contain 40%-50% oxygen, their direct use as conventional fuel is ruled out. Thus, we are focusing on our target in the production of bio-oil by fast pyrolysis of biomass, and the catalytic steam reforming of bio-oil to hydrogen-rich syngas (bio-oil-syngas) and catalytic conversion of the syngas to clean liquid bio-fuels by Fischer-Tropsch synthesis.

Several results have been reported about the production of hydrogen and hydrogen-rich syngas via steam reforming of bio-oil [9-12]. Conventional steam reforming catalysts are 10%-33% NiO on a mineral support [13] which operates at about 850 °C and the reforming S/C ratio (the molar ratio of steam to carbon fed) is usually 4-6. In our previous work [14,15], we found that MgO doped C12A7-O^- has good activity for catalytic steam reforming of bio-oil. The conversion efficiency of bio-oil (the carbon conversion and the yield of hydrogen) over the MgO doped C12A7-O^- catalyst is close to that over the Ni-based catalysts, but the MgO doped C12A7-O^- catalysts possess some advantages including longer lifetime and the fact that it is a non-noble metal catalyst. The composition of syngas derived from steam reforming reaction of bio-oil is much different from the conventional syngas used in industry. The latter mainly consists of H_2 and CO with a small amount of CO_2, whereas bio-oil-syngas generally

*Author to whom correspondence should be addressed. E-mail: liqx@ustc.edu.cn

consists much more amount of CO_2, resulting in higher CO_2/CO ratio. The composition of bio-oil-syngas also depends on the parameters of steam reforming reactions such as temperature, S/C ratio and catalyst types, etc. Generally, the adjusted bio-oil-syngas with composition of $H_2/(2CO+3CO_2)>1.0$ should be more favorable for FTS processes [16], which can be tailored in the downstream process by methane reforming (converts CH_4 with steam to CO and H_2), water-gas shift reaction (adjusts the H_2/CO ratio by converting CO with steam to H_2 and CO_2) and CO_2 removal, etc. However, the capital cost for syngas generation will be very high considering the adjusting steps. Therefore, simplification in the syngas production would significantly improve the overall process economics. A new possible way is the direct employment of bio-oil-syngas for the production of F-T hydrocarbons via one-pass through the reactor with using unconverted syngas co-produce electricity in a gas turbine combined cycle.

The obtained bio-oil-syngas consists mainly of H_2, CO, CO_2, and a small quantity of methane. Methane was most likely formed by the thermal cracking of oxygenated organic compounds, which always accompanies the catalytic reforming reaction. Methane in the bio-oil-syngas can be considered to be inert gas in the F-T synthesis reactor. The existence of methane in the syngas decreases the effective partial pressure of H_2, CO, and CO_2. To simplify the synthesis process, the model syngas was made, consisting only of H_2, CO, CO_2, and a small amount of N_2. N_2 acts as a balance gas for the calculation of mass balance, because N_2 is neither consumed nor produced under the reaction conditions. According to experiment results of bio-oil steam reforming [14,15], the gas mixture of $H_2/CO/CO_2/N_2$ (62/8/25/5, vol%) was taken as model bio-oil-syngas.

The Fischer-Tropsch synthesis (FTS) reaction, $CO+H_2$=hydrocarbon+H_2O, was found by Fischer and Tropsch in 1925 [17]. It can produce liquid fuels such as gasoline and diesel oil from coal or natural gas. The interest in FT synthesis has revived in recent years as a consequence of environmental demands and an increase in the known reserves of natural gas. Compared to conventional fuels (gasoline and diesel), FT fuels contain no sulfur and low aromatics. Furthermore, FT fuels may be suitable as hydrogen source for fuel cell vehicles (FCVs) via on-board reforming, because it is free of fuel cell catalyst poisons (e.g. sulphur). Some recent studies indicated that the use of Fischer-Tropsch (FT) technology for biomass conversion via the biomass gasification to synthetic hydrocarbons may offer a promising and carbon neutral alternative to conventional diesel, kerosene and gasoline [18-20].

The conventional FT process involves the synthesis of hydrocarbon fuels from a CO/H_2 mixture (syngas) over iron- or cobalt-based catalysts. For the FTS using the bio-oil-syngas, it is very important to select an optimum catalyst to obtain higher total carbon ($CO+CO_2$) conversion and higher C_{5+} selectivity. Although cobalt-based catalysts are nowadays the most used in industrial plants, with cobalt catalysts CO_2 is neither formed nor produced during FT synthesis and also neither strongly adsorbed nor hydrogenated, thus playing the role of a diluting gas [21]. The use of iron-based samples as catalysts in the FTS is very attractive due to their low cost, their high activity of FTS and high water gas shift reaction activity. Besides, iron-based catalysts are attractive because of the highly olefinic nature of the obtained products, which allows their use as a feedstock for chemical industry. In commercial FT fixed bed reactors, coprecipitated iron catalysts have usually been employed [22,23]. However, the catalysts should be readjusted to CO_2-rich and H_2-deficient feed gas so that the bio-oil-syngas can be directly used as a feed for hydrocarbon synthesis.

It is well known that the stronger bases of the group IA metals, especially potassium, are essential promoters in iron catalysts for FTS. The effect of potassium on the activity and product selectivity has been studied over a variety of iron-based catalysts [24-32]. In the CO hydrogenation reaction, the effect of potassium promotion on iron catalysts for FTS include (i) an increase in the average molecular weight (chain length) of hydrocarbon products (i.e., decrease in production of methane and light gases products), (ii) an increase in olefin selectivity, (iii) an increase in activity for the water gas shift (WGS) reaction and reverse water gas shift (RWGS) reaction, and (iv) an increase in FTS activity at low potassium concentrations, followed by decrease at higher levels of promotion [33]. Recent years, the K promotion in Fe based catalysts was found to be very essential for good catalytic performance in the hydrogenation of CO_2 [34-36]. It should be pointed out that bio-oil-syngas contains CO and CO_2, the FTS using bio-oil-syngas will convert CO and CO_2 simultaneously to hydrocarbon. The purpose of this work is not only to investigate the effect of potassium on coprecipitated Fe/Cu/Al/K catalysts for bio-fuel synthesis from bio-oil-syngas but also to select the optimal potassium content for FTS using CO_2-rich and H_2-deficient syngas from bio-oil steam reforming.

II. EXPERIMENTS

A. Catalysts preparation

The Fe/Cu/Al/K catalysts were prepared by using a continuous precipitation method. The catalyst precursor was precipitated from an aqueous solution containing iron, copper and aluminum nitrates at the desired Fe/Cu/Al ratio (100Fe/6Cu/16Al, weight ratio) using aqueous ammonia at the constant pH of 7.0 and the constant temperature of 80 °C. The obtained precipitation was filtered and washed three times by distilled water, then dried at 110 °C for 24 h in a vacuum oven. After the drying step, the potassium promoter was added as

DOI:10.1088/1674-0068/21/02/141-150

aqueous $KHCO_3$ solution via an incipient wetness pore-filling technique. The final step was to dry the catalysts at 110 °C for 24 h in a vacuum oven and then calcine the catalysts at 450 °C for 6 h. The calcined catalysts were crushed and sieved to 0.2-0.3 mm. These series catalysts were defined as 100Fe/6Cu/16Al/xK (x=0, 2, 4, 6, 8, 10, 12, weight ratio).

B. Catalyst characterization

X-ray diffraction (XRD) measurements were employed to investigate the structure of the catalysts before and after the steam reforming experiments. The catalysts are generally crushed into powder with the average diameter of 20-30 μm. Powder X-ray diffraction patterns were recorded on an X'pert Pro Philips diffractometer with a Cu Kα source. The measurement conditions were in the 2θ range of 10°-80°, step counting time of 5 s, and step size of 0.017° at 298 K.

The Brunauer-Emmett-Teller (BET) surface area of the catalyst was determined by N_2 physisorption at 77 K using a COULTER SA 3100 analyzer.

The X-ray photoelectron spectroscopy (XPS) measurements were performed on a VG ESCALAB MKII instrument, using Mg Kα primary radiation (15 keV, 10 mA). The normalized XPS intensities, which are proportional to the effective concentrations of the corresponding elements in the surface layer, were determined as the integrated peak area divided by their corresponding sensitivity factor. The C1s peak was used as a calibration standard for determining the peaks' position and the elemental concentration.

The basic property of the 100Fe/6Cu/16Al/xK catalysts (weight ratio) catalyst were characterized using the temperature programmed desorption of CO_2 (CO_2 TPD). The experiments were performed using a quartz-made microreactor with 200 mg catalyst. The catalysts were reduced *in situ* in hydrogen at 400 °C for 12 h. The samples were flushed with argon at 400 °C for 0.5 h and cooled to 30 °C. After this pretreatment, the pretreated samples were saturated with CO_2 at room temperature for 30 min (20 mL/min). Then the samples were flushed with Ar flowing at 20 mL/min for 30 min, afterwards the temperature was increased to 800 °C at a heating rate of 10 °C/min. Gas that desorbed was monitored using a mass spectrometer (Balzers, GSD 300 OmniStar).

C. Measurements of activity and selectivity

The FTS was investigated in a 1 cm i.d. stainless steel fixed bed flow reactor (Fig.1). The calcined catalyst (1.5 g) was loaded in the reactor and diluted with inert silica sand of the same particle size. The volume ratio of catalyst to silica sand was 1:8. Thus, a uniform gas flow at low pressure drop could be achieved, and the high degree of catalyst dilution with the inert material allowed for operation at almost isothermal conditions [37]. The catalyst precursor was reduced in situ in a flow of ultra-high purity hydrogen at 400 °C for 12 h under 0.3 MPa. The flow rate of hydrogen was maintained at 90 mL/min. After the temperature was cooled down to the reaction temperature, the bio-oil-syngas was fed into the reactor. The reaction temperature was measured by a thermocouple inserted into the catalyst bed. The feed gas and reducing gas were individually metered and controlled with commercial mass flow controller.

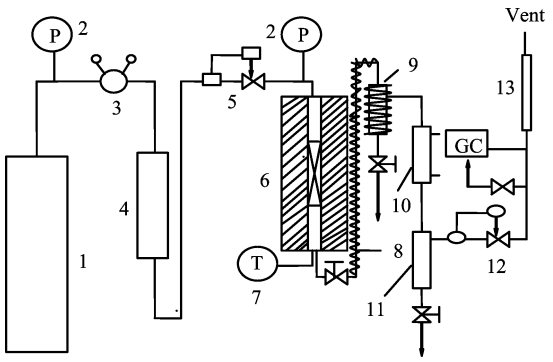

FIG. 1 Schematic diagram of experimental apparatus for Fischer-Tropsch synthesis using the bio-oil-syngas. 1. Bio-oil-syngas, 2. Pressure gauge, 3. Pressure regulator (YT-2), 4. Gas purifier, 5. Mass flow controller, 6. Fixed bed reactor, 7. Thermocouple, 8. Electric heating strip, 9. Wax collector, 10. Water-cool vessel, 11. Liquid product condenser, 12. Back pressure regulator, 13. Soap flowmeter.

D. Products analysis and kinetic parameters formulae

Gaseous products and reactants were analyzed with two on-line gas chromatographs (SP6800-A). H_2, N_2, CO, CO_2, and CH_4 were analyzed on the thermal conductivity detector (TCD) after separation by a carbon molecular sieve column (TDX-01), using argon as carrier gas. Light hydrocarbons (C_1-C_4) were separated by a Porapack-Q column and detected on the flame ionization detector (FID). The analysis of CH_4 was used as the link to correlate the peaks of FID and TCD. C_{5+} hydrocarbons were analyzed by a capillary column (SE-30, uniport). The reactants conversions and the products selectivities were calculated by the following formula:

$$X_{\text{reactant}}(\%) = \frac{a_{\text{in}} - a_{\text{out}}}{a_{\text{in}}} \times 100\% = \frac{(\text{reactant}/N_2)_{\text{in}} - (\text{reactant}/N_2)_{\text{out}}}{(\text{reactant}/N_2)_{\text{in}}} \times 100\% \quad (1)$$

a_{in} is moles of reactant$_{\text{in}}$, a_{out} is moles of reactant$_{\text{out}}$. Reactant stands for CO, CO_2, and total carbon ($CO+CO_2$).

$$S_{CH_4}(\%) = \frac{b}{c_{\text{in}} - c_{\text{out}}} \times 100\% \quad (2)$$

DOI:10.1088/1674-0068/21/02/141-150

$$S_{C_n}(\%) = \frac{n \times d}{c_{in} - c_{out}} \times 100\% \quad (3)$$

b is moles of $CH_{4produced}$, c_{in} and c_{out} are moles of $(CO+CO_2)_{in}$ and moles of $(CO+CO_2)_{out}$ respectively, d is $C_{nproduced}$ stands for hydrocarbon that contains n carbon number, n=2, 3, 4.

$$S_{C_{5+}}(\%) = 100\% - \sum(S_{CH_4} + S_{C_2} + S_{C_3} + S_{C_4}) \quad (4)$$

III. RESULTS AND DISCUSSION

A. Effects of potassium content on reactants' conversion

Figure 2 shows the effect of potassium content of 100Fe/6Cu/16Al/xK on the CO conversion, the CO_2 conversion, and the total carbon ($CO+CO_2$) conversion using the model bio-oil-syngas at 300 °C, 1.5 MPa and contact time of 12.5 g_{cat}h/mol (the contact time, described by W/F, W: weight of catalyst, F: mole flow rate of the model syngas). When 100Fe/6Cu/16Al/0K was used as catalyst, the CO conversion of 44.2% and the CO_2 conversion of 14.5% were obtained. After potassium was added to the iron catalyst, it was found that the CO conversion prominently increases to 60% and the CO_2 conversion increases to 20% with x value of 100Fe/6Cu/16Al/xK increasing from 0 to 2. With further increasing x value from 2 to 6, the CO conversion increases smoothly and reaches a maximum (65%) and the CO_2 conversion also reaches a maximum of 23%. Further increase of potassium content (x>6) leads to a slight decrease of CO and CO_2 conversion. The total carbon ($CO+CO_2$) conversion has the similar trend with CO and CO_2 conversion with increasing of K content. The CO hydrogenation via the FTS reaction can be recognized as a polymerization reaction with the basic steps of: (i) reactant (CO) adsorption on the catalyst surface, (ii) chain initiation by CO dissociation followed by hydrogenation, (iii) chain growth by insertion of additional CO molecules followed by hydrogenation, (iv) chain termination, and (v) product desorption from the catalyst surface [38].

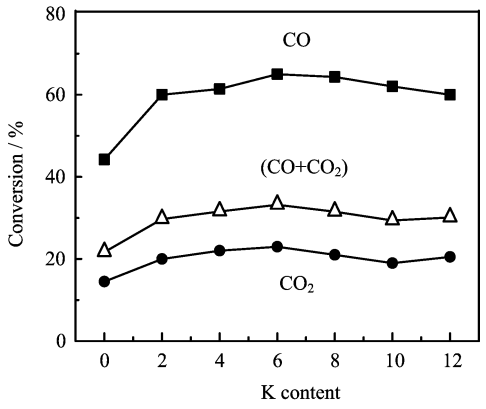

FIG. 2 Effect of potassium content on CO conversion, CO_2 conversion, and total carbon ($CO+CO_2$) conversion over 100Fe/6Cu/16Al/xK catalysts.

Chemisorbed methyl species are formed by dissociation of absorbed CO molecules and stepwise addition of hydrogen atoms. These methyl species can further hydrogenate to form methane or act as initiators for chain growth to form hydrocarbons. Overall the FTS reaction via the CO hydrogenation over Fe-based catalysts would be represented by the reaction of $2CO+H_2 \rightarrow -CH_2^- - +CO_2$. It should be pointed out that the considerable amount of CO_2 contained in the bio-oil-syngas. About CO_2 hydrogenation to hydrocarbons, a two steps' mechanism has been put forward [39]:

$$CO_2 + H_2 \rightarrow CO + H_2O \quad (5)$$
$$\Delta_R H^o_{300} = 38 \text{ kJ/mol}$$
$$CO + H_2 \rightarrow -CH_2^- - + H_2O \quad (6)$$
$$\Delta_R H^o_{300} = -166 \text{ kJ/mol}$$

The first step is RWGS reaction, which converts CO_2 to CO and the subsequent step is CO hydrogenation to hydrocarbons via FTS, with CO being the intermediate. For potassium promoted iron catalysts, it was found that potassium promotion increases CO chemisorption and decreases H_2 chemisorption in CO hydrogenation. This was explained by the fact that potassium donates electrons to iron, facilitating CO chemisorption, since CO tends to accept electrons from iron. On the other hand, hydrogen at higher surface coverages donates electrons to iron (electron affinity decreases upon H_2 chemisorption), and the presence of electron-donating alkali would be expected to weaken the iron-hydrogen bond.

The net result of potassium promotion is a strengthening of the Fe−C bond and weakening of the C−O and Fe−H bonds. The promotional effect of potassium on CO_2 hydrogenation can be explained by the effect of potassium on both RWGS and F-T reactions. Addition of potassium to iron catalysts resulted in a marked increase in the heat of CO_2 adsorption at all coverages and in the increase in CO adsorption heat at low coverages, while potassium decreases the initial heats of hydrogen adsorption. Meanwhile, potassium is a strong base. CO_2 appears to chemisorb not only on the surface of iron, but also on potassium oxide.

It is postulated that potassium enhanced both the strength and coverage of CO_2 adsorption on the catalyst surface that consequently led to an increase in CO_2 conversion [35]. The increase of CO and CO_2 conversion with potassium content increasing in the range of x<6 could be related to the enhancement of CO_2 and CO adsorption and dissociation by potassium promotion. The subsequent diminution of the activity in the range of x>6 may be caused by the coverage of Fe active sites with potassium. It was also noticed that the variation in the CO_2 conversion (14.5%-23%) was not pronounced with the variation of potassium content, which seems

DOI:10.1088/1674-0068/21/02/141-150

to be a characteristic behavior for CO_2 hydrogenation. This could be related to an inhibition effect of the water produced. This effect could be very important for CO_2 hydrogenation because more amount of water formed in CO_2 hydrogenation reaction than in CO hydrogenation reaction.

B. Effects of potassium content on hydrocarbon products selectivity

Generally, the FT reaction produces hydrocarbons of variable chain length. Higher liquid hydrocarbon selectivity (C_{5+} selectivity) is necessary to obtain a maximum amount of long hydrocarbon chains. Selectivity of the hydrocarbons (product distribution) is influenced by a number of factors, either catalyst dependence (type of metal (iron or cobalt), support, preparation, preconditioning and age of catalyst) or non-catalyst dependence (composition of the feed gas, temperature, pressure, W/F and reactor type) [40].

For coprecipitated iron catalysts, potassium promoter has pronounced influence on hydrocarbon product distribution. The effect of potassium content on the selectivity of hydrocarbon products is presented in Fig.3. With x value increasing from 0 to 6, CH_4 selectivity shows a very prominent decrease from 33% to 16.4% and C_2-C_4 hydrocarbon selectivity also decrease from 51% to 35.5%. Further increasing the potassium content (x>6) leads to the slightly decrease of CH_4 selectivity from 16.4% to 13.1% and C_2-C_4 selectivity from 35.5% to 30.7%. On the contrary, the desired C_{5+} selectivity increases from 16% to 48.1% with the increasing of x value from 0 to 6. The C_{5+} selectivity further increases to 55.8% when x value increases to 12. On the other hand, the olefin selectivity in C_2-C_4 prominently increases from 38% to 77% with x increasing from 0 to 6, and further to increase the x value from 6 to 12 leads to the slight increase of the olefin selectivity in C_2-C_4. The small changes of CH_4, C_2-C_4, and C_{5+} selectivity observed for potassium content between 6-12 suggest

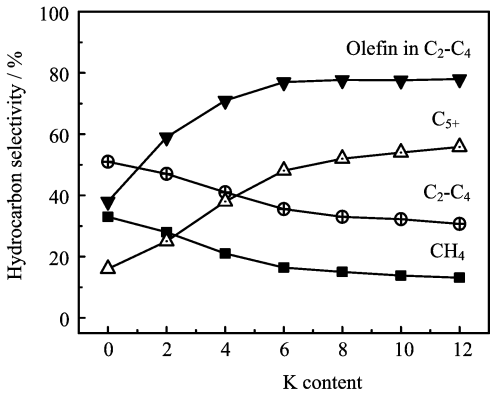

FIG. 3 Effect of potassium content on the selectivity of hydrocarbon products over 100Fe/6Cu/16Al/xK catalysts.

that in this case the maximum interaction between Fe-K must occur for potassium content close to 6. The changes of hydrocarbon products selectivities with different K content are consistent with the change of the C/H ratio on the catalyst surface.

It is well known that potassium promotion increases CO chemisorption and decreases H_2 chemisorption (strengthening of the Fe−C bond and weakening of the C−O and Fe−H bonds). When bio-oil-syngas was used, with the increase of potassium content in the Fe/Cu/Al/K catalyst, carbon oxide (CO and CO_2) chemisorption will increase and H_2 chemisorption decrease at the same time. Thus, C/H ratio on the catalyst surface increases with the increase of K content of iron catalyst. With regards to the hydrocarbon distribution, it is easily understood that selectivity toward gas phase hydrocarbon fraction (C_1-C_4) decreased while selectivity to C_{5+} increased with potassium content. As for the olefin selectivity in the hydrocarbon product, it is well established that the olefin selectivity depends not only on the primary olefin selectivity in FTS but also on the activity of secondary hydrogenation of the primary product. Both steps are related to the adsorbed C/H ratio on the catalyst surface. The higher the surface C/H ratio will lead to the lower the saturation degree of the product. Consequently, a secondary reaction of olefin hydrogenation was inhibited, and the olefin selectivity in C_2-C_4 hydrocarbon increased.

C. Effects of potassium content on the hydrocarbon products distribution

The effect of potassium content on hydrocarbon products distribution is presented in Fig.4. As can be seen, with the increasing of potassium content, hydrocarbon selectivity shifts to longer chain product (C_{5+}) and gas phase product selectivity (CH_4 and C_2-C_4) decreases. FTS is kinetically controlled and the intrinsic kinetics is stepwise chain growth, in effect the polymerization of CH_2 groups on a catalyst surface. FTS products selectivities are determined by the ability of a catalyst to catalyze chain propagation *versus* chain termination reactions. The polymerization rate, and therefore kinetics, is independent of the products formed. The probability of chain growth and chain termination is independent of chain length. The effect of potassium addition on hydrocarbon selectivity observed in the present study is in agreement with the results obtained in several earlier studies with a variety of iron catalysts [25,31,41]. The increase in average molecular weight of hydrocarbon products is due to the increase carbon oxide (CO and CO_2) and lower H_2 surface coverage in the presence of potassium. Since, chain termination results from the hydrogenation of the iron-carbon bond and the presence of potassium enhances the probability of continued chain growth, i.e., formation of higher molecular weight products [42].

DOI:10.1088/1674-0068/21/02/141-150

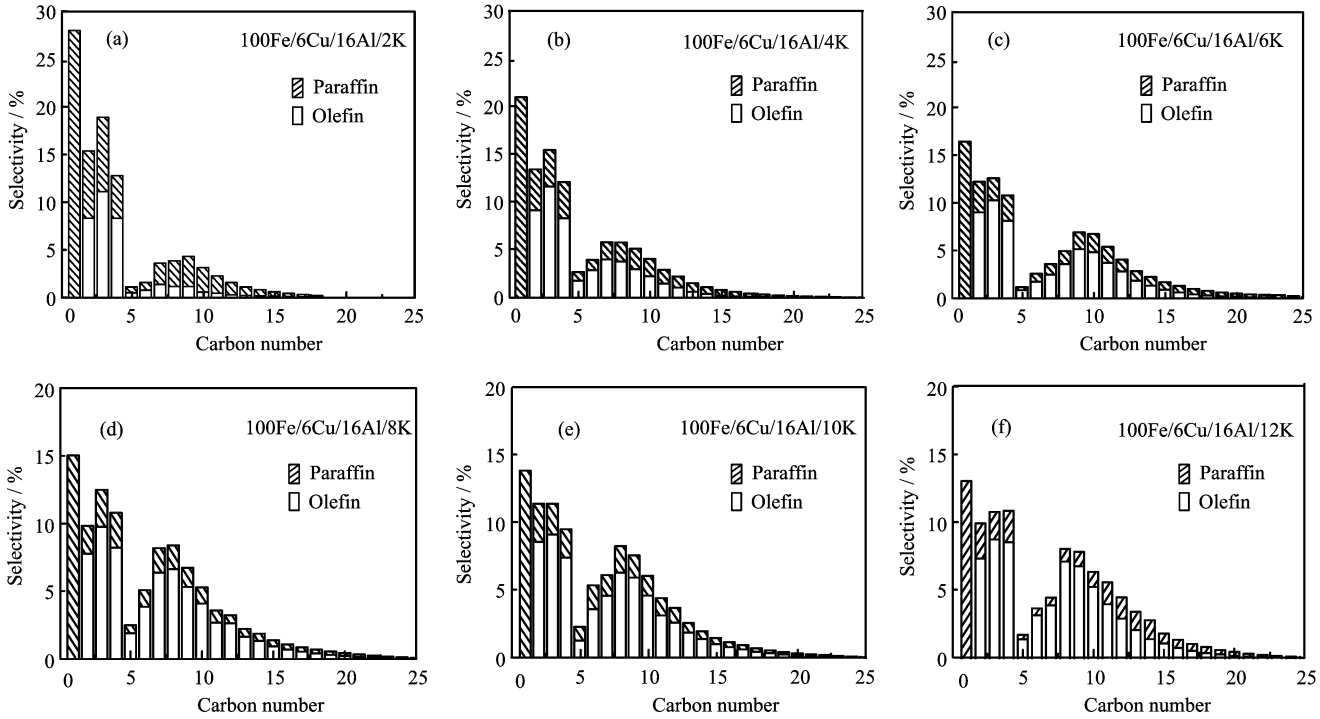

FIG. 4 The effect of potassium content on hydrocarbon products distribution over 100Fe/6Cu/16Al/xK (x=2-12) catalysts.

D. Effect of time on stream

The effects of time on stream on the total carbon (CO+CO_2) conversion using Fe/Cu/Al/K catalysts with different K contents are depicted in Fig.5. It was found that 100Fe/6Cu/16Al/0K has the lowest initial activity for CO and CO_2 hydrogenation. With increasing of potassium content in 100Fe/6Cu/16Al/xK catalysts, the initial activity of iron catalysts for CO and CO_2 hydrogenation increase. This indicates that potassium plays an important role in the iron catalysts. It is a general understanding that iron carbides on the surface of iron catalyst are active species of the Fischer-Tropsch reaction. Iron carbides were formed by the reaction of iron and chemisorbed carbon (C_{ads}), which derives from the decomposition reaction of CO, namely, $2CO=CO_2+C_{ads}$. Potassium promotion increases CO chemisorption and promotes the formation of iron carbides. Potassium addition also increases CO_2 chemisorption and promotes CO formation via the RWGS reaction ($CO_2+H_2\rightarrow CO+H_2O$). It was also found that the total carbon (CO+CO_2) conversion was stable for 80 h with increasing x value from 2 to 6. Beyond the ratio (x>6), the total carbon (CO+CO_2) conversion decreased with the increasing of time on stream. It is suggested that too high K promotion led to the gradual deactivation of the catalysts, due to carbon deposition on the surface of the catalyst. It is desirable, therefore, to select a K content of x=6 as an optimum catalyst composition for the reaction of bio-oil-syngas.

E. Effect of CO_2/(CO+CO_2) on FTS

Generally, the syngas derived from bio-oil via catalytic steam reforming is a CO_2-rich syngas. The volume ratio of $H_2/CO/CO_2$ in the syngas mainly depends on the types of reforming catalyst, reforming temperature, S/C ratio, etc. In addition, the composition of bio-oil-syngas can be adjusted by the combination of methane reforming, RWGS reaction and CO_2 removal before the synthesis loop. The CO_2/(CO+CO_2) ratio will be variable depending on reforming condition and the combination method. In this work, we investigated the FTS reaction by varying the CO_2/(CO+CO_2) ratio of the syngas at 300 °C, 1.5 MPa, H_2:(CO+CO_2)=1.87, and W/F=12.5 g_{cat}h/mol (see Table I). For the syngas of H_2/CO (i.e., r=0), the CO conversion reached about 95%, and the highest total carbon conversion about 64.1% was obtained. It should be pointed out that 30.9% carbon of the total carbon convert to CO_2 via the water-gas shift reaction over the Fe/Cu/Al/K catalyst when H_2/CO (r=0) was used as syngas. With increasing the r value to 0.5, CO conversion slightly decreases to 89% and CO_2 conversion remains very low (<9%). The above results indicate that CO hydrogenation is the preferred reaction up to the r value of 0.5. Further increasing the r value to 0.76, CO conversion smoothly decreases to 72.5%. On the other hand, CO_2 conversion increases from 8.9% to 29.2% with r increasing from 0.5 to 1. When H_2/CO_2 (r=1) is used as syngas, according to the two steps' mechanism, CO is produced as an intermediate via RWGS reaction. It was

DOI:10.1088/1674-0068/21/02/141-150

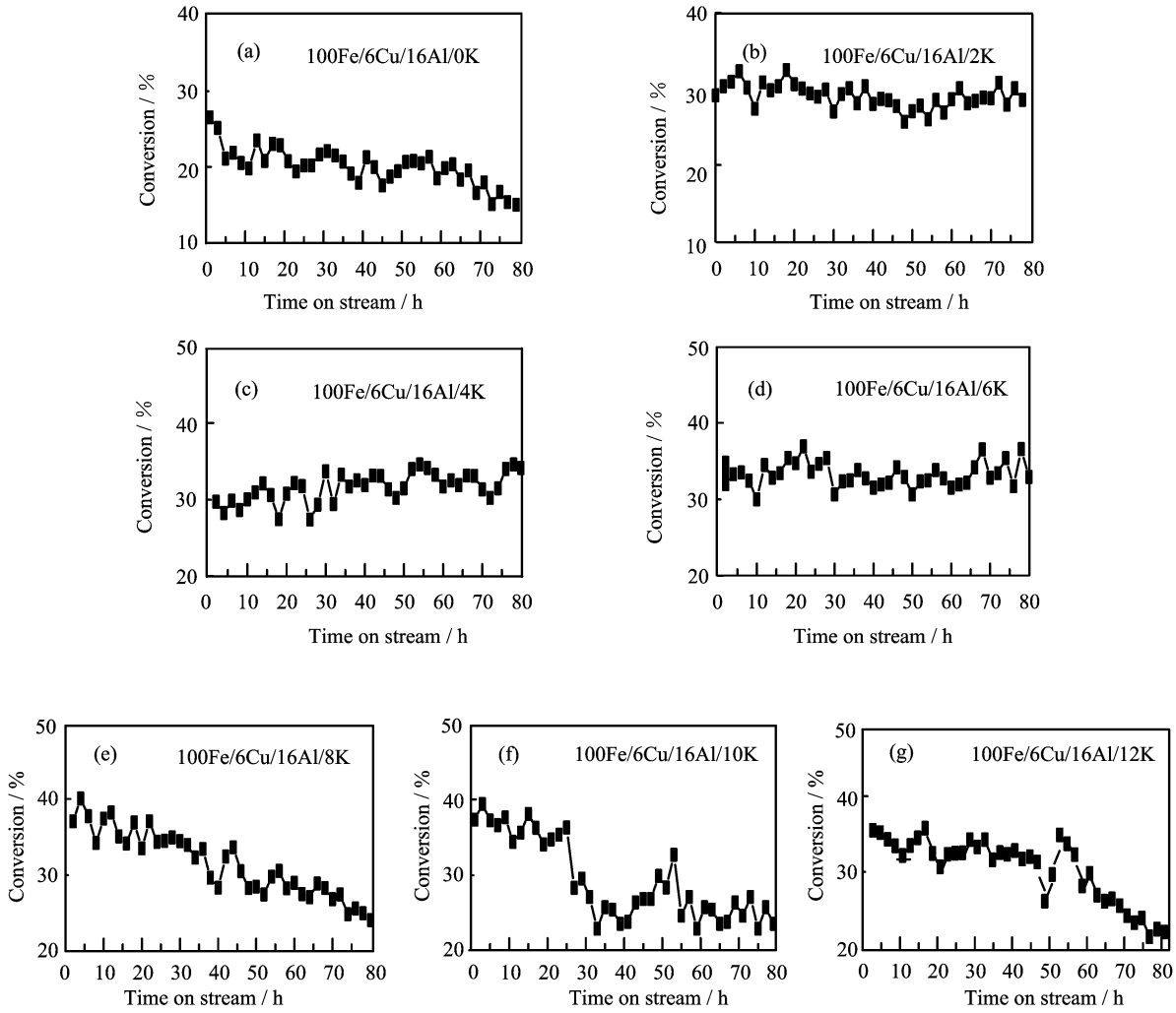

FIG. 5 Effect of time on stream on the total carbon ($CO+CO_2$) conversion using 100Fe/6Cu/16Al/xK (x=0-12) catalysts with different K content.

TABLE I The effect of $CO_2/(CO+CO_2)$ on CO, CO_2, total carbon conversion, and CH_4, C_{5+} selectivity over 100Fe/6Cu/16Al/6K catalyst

$CO_2/(CO+CO_2)$	Conversion/%			Selectivity/%	
	CO	CO_2	Total carbon	CH_4	C_{5+}
0.0	95	–	64.1	16	49.2
0.5	89	8.9	49	16	47.4
0.76	72.5	24	35.8	17.4	44.2
1.0	–	29.2	21.9	18	43.4

found that 7.3% of total carbon in H_2/CO_2 converts to CO in the effluent from FT reactor. The total carbon conversion smoothly decreases from 64.1% (H_2/CO as syngas) to 21.9% (H_2/CO_2 as syngas) in the all investigated range. On the other hand, with the increasing of $CO_2/(CO+CO_2)$ ratio, it is found that there is no prominent influence of r value on CH_4 and C_{5+} selectivity. This indicates that $CO_2/(CO+CO_2)$ ratio mainly affects the conversion efficiency of the carbon oxide (CO and CO_2) and the rate of CO_2 hydrogenation is about 3 times lower than that of CO hydrogenation.

F. Catalyst characterization

The amount of CO_2 desorbed from coprecipitated 100Fe/6Cu/16Al/xK catalysts (x=0, 6, 12) is determined by the CO_2 TPD measurements. As can been seen from Table II, when 100Fe/6Cu/16Al/0K was used

DOI:10.1088/1674-0068/21/02/141-150

TABLE II The effect of potassium content on CO_2 uptake of coprecipitated 100Fe/6Cu/16Al/xK catalysts (x=0, 6, 12)

Catalysts	CO_2 uptake/(μmol/g_{cat})
100Fe/6Cu/16Al/0K	114.5
100Fe/6Cu/16Al/6K	254.3
100Fe/6Cu/16Al/12K	381.6

as catalyst, CO_2 uptake was 114.5 μmol/g_{cat}. With the increasing of potassium content, CO_2 uptake increases prominently. This indicates that when potassium is added to the iron catalyst, the amount of basic sites on the catalyst surface increases. It has been reported that a higher surface basicity of the iron catalyst correlates with a high carbon conversion and lower methane selectivity in the FTS [27]. It also agree with our observation.

In this work, five different samples are measured by XRD to investigate the structure characteristics of 100Fe/6Cu/16Al/xK catalysts. It is well known that the iron element of coprecipitated iron catalyst exists mainly as hematite phase. By comparing the peak positions and intensities of the XRD pattern with the data in the JCPDS cards, we can't find visible peaks of the iron oxide species in all XRD patterns. It implies that the iron oxide species is therefore present as either small particles (considering the XRD detection limit: <3 nm) or it is amorphous. Similarly, as potassium was added to the coprecipitated iron catalyst, we have not observed the obvious diffraction peaks of K_2CO_3. Thus, potassium is well dispersed on the surface of 100Fe/6Cu/16Al/xK via the incipient wetness pore-filling technique. Moreover, 100Fe/6Cu/16Al/6K and 100Fe/6Cu/16Al/12K after 80 h activity test were measured by X-ray diffraction (XRD) to investigate the structure change of 100Fe/6Cu/16Al/xK (weight ratio) catalysts. As can be seen in Fig.6, the Fe phase of the catalysts consist of the Hägg carbide (x-Fe_5C_2) and magnetite (Fe_3O_4). The diffraction peak around 36° corresponds to Fe_3O_4 and the diffractions between 39°-50° are due to x-Fe_5C_2. The peaks of x-Fe_5C_2 are indexed at 2θ=43.45°, 44.15°, and 45°, as reported by Niemantsverdriet [43], Senateur [44] and JCPDS file [45]. The Fe_3O_4 phase in the catalysts has been known as an active phase in water-gas shift reaction and x-Fe_5C_2 has been known as an active phase in F-T reaction [46].

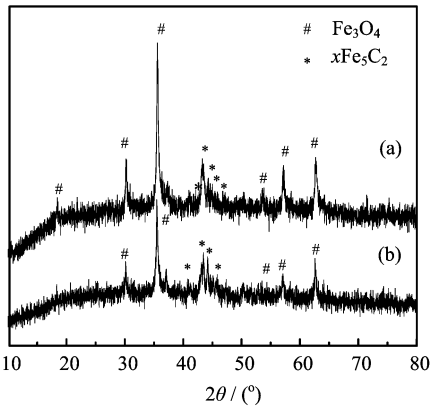

FIG. 6 XRD patterns of (a) 100Fe/6Cu/16Al/12K and (b) 100Fe/6Cu/16Al/6K after activity test of 80 h.

The surface content (mol%) of Fe and K of 100Fe/6Cu/16Al/xK (x=0, 4, 6, 8, 12) is confirmed by the XPS and presented in Fig.7. As can be seen, potassium content on surface of the iron catalysts increases almost proportionally with the increasing of x value. At the same time, iron content on the surface of the catalysts decreases with the increasing of x value. This indicates that potassium addition to the coprecipitated iron catalyst will partly mantle the iron species on the catalyst surface. Based on the results, we can draw a conclusion that potassium added by the incipient wetness pore-filling technique is mainly dispersed on the surface or in the micro-pores of the catalysts. Moreover, the BET surface areas of 100Fe/6Cu/16Al/xK (x=0, 4, 6, 8, 12) catalysts are depicted in Fig.8. As can be seen, 100Fe/6Cu/16Al/0K has a maximum BET surface area of 125 m^2/g in our investigated catalysts. The

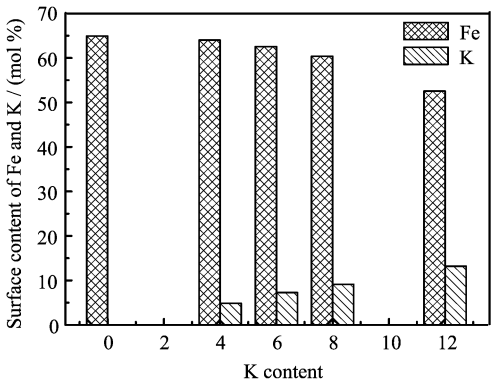

FIG. 7 The effect of potassium content (x value, x=0, 4, 6, 8, 12) on the surface content (mol%) of Fe and K.

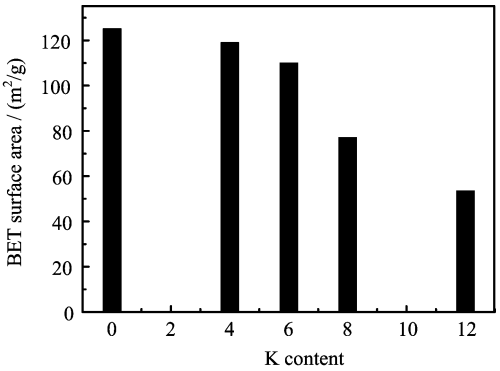

FIG. 8 The effect of potassium content on the BET surface area of the 100Fe/6Cu/16Al/xK (x=0, 4, 6, 8, 12).

DOI:10.1088/1674-0068/21/02/141-150

BET surface areas slightly decrease to 110 m^2/g when x value increases from 0 to 6. More content of potassium (x>6) leads to sharply decrease of the BET surface area of 100Fe/6Cu/16Al/xK catalyst. When x value comes up to 12, the minimum value of the BET surface area about 53.5 m^2/g is obtained. The decrease in surface area of the potassium-promoted catalysts may be attributed to the pore filling or pore blocking of part of the micro-pores by potassium during the impregnation step. Thus, x=6 will be the optimum value to obtain higher BET surface area and higher catalytic activity.

Carbon species on 100Fe/6Cu/16Al/6K and 100Fe/6Cu/16Al/12K catalysts' surface after 80 h reaction are confirmed by the XPS and presented in Table III. As can be seen from Table III, carbon element on the catalysts' surface mainly exists as carbide and carbon deposition. It was also found that with the increasing of potassium content, carbon deposition increases. This indicates that high potassium content will increase the carbon deposition and catalyst deactivation rate.

TABLE III The effect of potassium content of coprecipitated 100Fe/6Cu/16Al/xK catalysts (x=6, 12) on carbon deposition after 80 h reaction

Catalysts	Carbide/%	Carbon deposition/%
100Fe/6Cu/16Al/6K	18.17	13.72
100Fe/6Cu/16Al/12K	12.66	25.53

IV. CONCLUSION

Fischer-Tropsch synthesis (FTS) using bio-oil-syngas via steam reforming of bio-oil was investigated as a potential and promising way to produce clean liquid biofuels. A suitable catalyst is necessary for F-T synthesis using CO_2-rich bio-oil-syngas to obtain higher carbon conversion (CO and CO_2 conversion) and higher C_{5+} selectivity. The effect of potassium addition to coprecipitated iron catalysts on carbon oxide (CO, CO_2, and total carbon) conversions and the selectivities of hydrocarbon products were investigated in a fixed bed flow reactor at 300 °C, 1.5 MPa and W/F of 12.5 g_{cat}h/mol. Based on experiment results and general catalyst characterization, 100Fe/6Cu/16Al/6K (weight ratio) was selected as the optimum catalyst for F-T synthesis from bio-oil-syngas. The CO conversion of 65%, the CO_2 conversion of 23% with the C_{5+} selectivity of 48.1% was obtained at a typical reaction of 300 °C, 1.5 MPa, W/F=12.5 g_{cat}h/mol with syngas of $H_2/CO/CO_2$=62:8:25. Potassium plays an important role in coprecipitated iron catalyst. It increases the catalytic activity of F-T synthesis and RWGS (Reverse Water-Gas Shift) reaction and the average molecular weight of hydrocarbon products. It also causes suppression of olefin hydrogenation and isomerization reactions. Reaction studies of the type presented in this work coupled with detailed catalyst characterization studies are needed to gain better understanding of the role of potassium promotion in iron catalysts for the Fischer-Tropsch synthesis.

V. ACKNOWLEDGMENTS

The authors thank Prof. Yi-lu Fu and Prof. Pei-yan Lin for their kind help. This work was supported by the 863 Program (No.2006AA05Z118), 973 Program (No.2007CB210206), and the National Natural Science Foundation of China (No.50772107).

[1] A. V. Bridgwater, Catal. Today **29**, 285 (1996).
[2] L. Garcia, M. L. Salvador, J. Arauzo, and R. Bilbao, J. Anal. Appl. Pyrol. **58-59**, 491 (2001).
[3] M. P. Aznar, M. A. Caballero, J. Corella, G. Molina, and J. M. Toledo, Energy & Fuels **20**, 1305 (2006).
[4] L. Garcia, M. L. Salvador, J. Arauzo, and R. Bilbao, Energy & Fuels **13**, 851 (1999).
[5] P. McKendry, Bioresource Technol. **83**, 47 (2002).
[6] S. Czernik and A. V. Bridgwater, Energy & Fuels **18**, 590 (2004).
[7] A. V. Bridgwater, D. Meier, and D. Radlein, Org. Geochem. **30**, 1479 (1999).
[8] J. Piskorz, D. S. Scott, D. Radlein, E. J. Soltes, and T. A. Milne, Eds., *ACS Symposium Series* 376, Washington: American Chemical Society, 167 (1988).
[9] D. Wang, S. Czernik, D. Montané, M. Mann, and E. Chornet, Ind. Eng. Chem. Res. **36**, 1507 (1997).
[10] D. Wang, S. Czernik, and E. Chornet, Energy & Fuels **12**, 19 (1998).
[11] L. Garcia, R. French, S. Czernik, and E. Chornet, Appl. Catal. A **201**, 225 (2000).
[12] S. Czernik, R. French, C. Feik, and E. Chornet, Ind. Eng. Chem. Res. **41**, 4209 (2002).
[13] C. N. Satterfield, *Heterogeneous Catalysis in Industrial Practice*, New York: McGraw-Hill, 427 (1991).
[14] Z. X. Wang, Y. Pan, T. Dong, X. F. Zhu, T. Kan, L. X. Yuan, Y. Torimoto, M. Sadakata, and Q. X. Li, Appl. Catal. A **320**, 24 (2007).
[15] Y. Pan, Z. X. Wang, T. Kan, X. F. Zhu, and Q. X. Li, Chin. J. Chem. Phys. **19**, 190 (2006).
[16] M. E. Dry, Appl. Catal. A **138**, 319 (1996).
[17] H. G. Olive and S. Olive, *The Chemistry of the Catalyzed Hydrogenation of Carbon Monoxide*, Tokyo: Springer-Verlag, 144 (1984).
[18] A. P. C. Faaij, C. N. Hamelinck, and M. Tijmensen, *Proceedings of the First World Conference on Biomass for Energy and Industry*, London: James & James Ltd., 687 (2001).
[19] E. D. Larson and H. Jin, *Proceedings of the Fourth Biomass Conference of the Americas*, Kidlington: Elsevier Science, 843 (1999).
[20] C. N. Hamelinck, A. P. C. Faaij, H. Uil, and H. Boerrigter, Energy **29**, 1743 (2004).

DOI:10.1088/1674-0068/21/02/141-150

[21] T. Riedel, M. Claeys, H. Schulz, G. Schaub, S. S. Nam, K. W. Jun, M. J. Choi, G. Kishan, and K. W. Lee, Appl. Catal. A **186**, 201 (1999).
[22] M. E. Dry, Catal. Today **6**, 183 (1990).
[23] D. B. Bukur, X. Lang, D. Mukesh, W. H. Zimmerman, M. P. Rosynek, and C. Li, Ind. Eng. Chem. Res. **29**, 1588 (1990).
[24] R. B. Anderson, *Catalyst for the Fischer-Tropsch Synthesis, In Catalysis*, Vol. IV, P. H. Emmett, Ed., New York: Van Nostrand-Reinhold, 29 (1956).
[25] R. B. Anderson; B. Seligman, J. F. Schultz, and M. A. Elliot, Ind. Eng. Chem. **44**, 391 (1952).
[26] H. Kölbel and H. Giehring, Brennstoff-Chem. **44**, 343 (1963).
[27] M. E. Dry and G. J. Oosthuizen, J. Catal. **11**, 18 (1968).
[28] H. P. Bonzel and H. Krebs, Surf. Sci. **109**, L527 (1981).
[29] M. E. Dry, *The Fischer-Tropsch Synthesis. In Catalysis Science and Technology I*, J. R. Anderson, and M. Boudart, Eds., New York: Springer-Verlag, 159 (1981).
[30] H. Arakawa and A. T. Bell, Ind. Eng. Chem. Process Des. Dev. **22**, 97 (1983).
[31] R. A. Dictor and A. Bell, J. Catal. **97**, 121 (1986).
[32] T. J. Donnelly and C. N. Satterfield, Appl. Catal. **52**, 93 (1989).
[33] D. B. Bukur, D. Mukesh, and S. A. Patel, Ind. Eng. Chem. Res. **29**, 194 (1990).
[34] P. H. Choi, K. W. Jun, S. J. Lee, M. J. Choi, and K. W. Lee, Catal. Lett. **40**, 115 (1996).
[35] S. R. Yan, K.W. Jun, J. S. Hong, M. J. Choi, and K. W. Lee, Appl. Catal. A **194-195**, 63 (2000).
[36] K. W. Jun, S. J. Lee, H. Kim, M. Choi, and K. W. Lee, Stud. Surf. Sci. Catal. **114**, 345 (1998).
[37] T. Riedel, G. Schaub, K. W. Jun, and K. W. Lee, Ind. Eng. Chem. Res. **40**, 1355 (2001).
[38] P. L. Spath and D. C. Dayton, *Preliminary Screening-Technical and Economic Assessment of Synthesis Gas to Fuels and Chemicals with Emphasis on the Potential for Biomass-Derived Syngas*, NREL/TP-510-34929, 94.
[39] M. Niemelä and M. Nokkosmäki, Catal. Today **100**, 269 (2005).
[40] M. J. A. Tijmensen, A. P. C. Faaij, C. N. Hamelinck, and M. R. M. Hardeveld, Biomass & Bioenergy **23**, 129 (2002).
[41] B. Schliebs, J. Gaube, and B. Bunsen, Phys. Chem. **89**, 68 (1985).
[42] M. E. Dry, T. Shingles, L. Boshoff, and G. J. Oosthuizen, J. Catal. **15**, 190 (1969).
[43] J. Niemantsverdriet, A. van der Kraan, W. van Dijk, and H. vander Baan, J. Phys. Chem. **84**, 3363 (1980).
[44] J. Senateur, Ann. Chim. (Paris) **2**, 103 (1967).
[45] W. F. McClune, M. E. Mrose, B. Post, S. Weissmann, and H. F. McMuridie, *JCPDS-International Centre for Diffraction Data file*, 20-509 (1979).
[46] J. F. Shultz, W. K. Hall, T. A. Dubs, and R. B. Anderson, J. Am. Chem. Soc. **78**, 282 (1956).

DOI:10.1088/1674-0068/21/02/141-150